Ultrasound Obstet Gynecol 2011; **37**: 450–457
Published online in Wiley Online Library (wileyonlinelibrary.com). **DOI:** 10.1002/uog.8880

Non-invasive pulsed cavitational ultrasound for fetal tissue ablation: feasibility study in a fetal sheep model

Y. KIM*, S. K. GELEHRTER†, C. G. FIFER†, J. C. LU†, G. E. OWENS†, D. R. BERMAN‡, J. WILLIAMS‡, J. E. WILKINSON§, K. A. IVES* and Z. XU*

**Department of Biomedical Engineering, University of Michigan, Ann Arbor, MI, USA; †Department of Pediatrics and Communicable Diseases, University of Michigan, Ann Arbor, MI, USA; ‡Department of Obstetrics and Gynecology, University of Michigan, Ann Arbor, MI, USA; §Department of Pathology, University of Michigan, Ann Arbor, MI, USA*

KEYWORDS: fetal therapy; histotripsy; non-invasive tissue ablation; pulsed cavitational ultrasound; therapeutic ultrasound

ABSTRACT

Objectives *Currently available fetal intervention techniques rely on invasive procedures that carry inherent risks. A non-invasive technique for fetal intervention could potentially reduce the risk of fetal and obstetric complications. Pulsed cavitational ultrasound therapy (histotripsy) is an ablation technique that mechanically fractionates tissue at the focal region using extracorporeal ultrasound. In this study, we investigated the feasibility of using histotripsy as a non-invasive approach to fetal intervention in a sheep model.*

Methods *The experiments involved 11 gravid sheep at 102–129 days of gestation. Fetal kidney, liver, lung and heart were exposed to ultrasound pulses (< 10 μs) delivered by an external 1-MHz focused ultrasound transducer at a 0.2–1-kHz pulse-repetition rate and 10–16 MPa peak negative pressure. Procedures were monitored and guided by real-time ultrasound imaging. Treated organs were examined by gross and histological inspection for location and degree of tissue injury.*

Results *Hyperechoic, cavitating bubble clouds were successfully generated in 19/31 (61%) treatment attempts in 27 fetal organs beneath up to 8 cm of overlying tissue and fetal bones. Histological assessment confirmed lesion locations and sizes corresponding to regions where cavitation was monitored, with no lesions found when cavitation was absent. Inability to generate cavitation was primarily associated with increased depth to target and obstructing structures such as fetal limbs.*

Conclusion *Extracorporeal histotripsy therapy successfully created targeted lesions in fetal sheep organs without significant damage to overlying structures. With further improvements, histotripsy may evolve into a viable technique for non-invasive fetal intervention procedures. Copyright © 2011 ISUOG. Published by John Wiley & Sons, Ltd.*

INTRODUCTION

Congenital abnormalities are the leading cause of infant mortality in the USA, accounting for more than 20% of all infant deaths[1]. Many of these anomalies require invasive surgery after birth; however, some conditions are amenable to fetal intervention procedures, which may be able to prevent disease progression or worsening of the fetal condition[2,3]. Currently available fetal treatments for congenital abnormalities include percutaneous balloon atrial septoplasty in hypoplastic left heart syndrome with restrictive atrial septum[4], fetoscopic obliteration of blood vessels in twin–twin transfusion syndrome[5] and open surgical debulking for rapidly growing fetal masses[6]. However, preterm labor, infection and premature rupture of membranes remain as risk factors with even minimally invasive procedures. Physical and practical limitations such as fetal size and the adequacy of available equipment exist for current approaches; this limits the timing of interventions and likely affects their success. Non-invasive interventional techniques, such as therapeutic ultrasound, may reduce risk for both mother and fetus while possibly allowing earlier intervention options which may have a greater impact on disease progression, and potentially yield improved outcomes.

Fetal interventions in animal models have been reported using high-intensity focused ultrasound (HIFU) as a thermal ablation method[7,8]. Histotripsy is a form of focused ultrasound therapy based on a different

Correspondence to: Y. Kim, Department of Biomedical Engineering, University of Michigan, 2200 Bonisteel Blvd, Ann Arbor, MI 48109, USA (e-mail: yohankim@umich.edu)

Accepted: 3 November 2010

mechanism in which high-intensity ultrasound pulses are applied to create controlled cavitation bubble clouds at the treatment focus. Through the rapid growth and collapse of the bubbles, targeted tissue is mechanically fractionated into subcellular debris[9,10]. The initiation of the cavitation process is a threshold phenomenon, with bubble clouds generated only when the focal acoustic pressure exceeds a certain level[11]. The hyperechoic nature of the cavitation bubbles permits the real-time monitoring of therapy progression using conventional ultrasound imaging, and resulting lesions are limited to the focal zones where the cavitating bubble clouds were generated. Previous experiments in adult or neonatal animals have shown that histotripsy can efficiently and accurately fractionate and remove tissue from heart[12,13], kidney[14] and prostate[15] *in vivo*. The purpose of this study was to demonstrate, for the first time, the feasibility of applying histotripsy to non-invasively create localized lesions in fetal organs in a sheep model.

MATERIALS AND METHODS

Experiments involved 11 gravid ewes, median gestation 115 days, range 102–129 days (full ovine gestation: 150 days) with 15 fetuses. Each ewe was first sedated with an intramuscular injection of diazepam (0.5–1 mL/kg) and intravenous propofol (4–6 mL/kg), followed by endotracheal intubation and inhalation of 1–3% isoflurane gas. Vital signs were monitored throughout the experiment. All procedures were reviewed and approved by the University Committee on Use and Care of Animals at the University of Michigan.

Once the ewe was anesthetized and secured on the table, the abdomen was shaved and a depilatory cream was applied to remove any remaining wool and improve ultrasound coupling. Preliminary ultrasound imaging was performed using a clinical ultrasound imaging system (Sonos 7500, Philips Electronics, Andover, MA, USA) with a 5-MHz curvilinear imaging probe (Model c3540, Philips Electronics) to determine the number and lie of the fetuses. The ewe was then positioned on her side or back to optimize acoustic windows for fetal targeting.

A 1-MHz focused ultrasonic transducer (Imasonic, Besançon, France) with an aperture of 100 mm and focal length of 90 mm was used as the therapeutic unit. To monitor the treatment, a 3-MHz phased array ultrasonic imaging probe (Model S3, Philips Electronics) was coaxially aligned through a center hole in the therapy transducer specifically designed to accommodate the probe. The focal location of the transducer with respect to the imaging probe's field of view was found prior to treatment by generating a cavitation cloud in degassed water and highlighting the region where hyperechoic activity was observed on the imaging screen. Following this procedure, a metal bowl with a center opening lined with clear plastic was coupled to the ewe's abdomen using LithoClear® acoustic transmission gel (Sonotech, Inc., Bellingham, WA, USA), and filled with degassed water. This set-up allowed continued ultrasound coupling through water even when the transducer (with a fixed focal distance) was centimeters above the maternal abdomen to target shallower targets. Degassed water was used to minimize the formation of reflective gas bubbles at the skin interface. The transducer unit was secured to a three-axis motorized system (Parker Hannifin, Rohnert Park, CA, USA) and positioned within the water bowl to place the transducer's focus on the targeted organ (Figure 1).

Sheep were exposed to 1-MHz ultrasound pulses with measured free-field peak rarefactional pressures of 10–16 MPa. The ultrasound pulses were 5 μs in duration (five cycles at 1 MHz) and separated by 1–5 ms (i.e. pulse repetition frequencies of 200 Hz to 1 kHz). The formation of a highly echogenic cavitation bubble cloud at the focus of the transducer during treatment allowed procedures to be monitored in real time, with the cavitating bubble

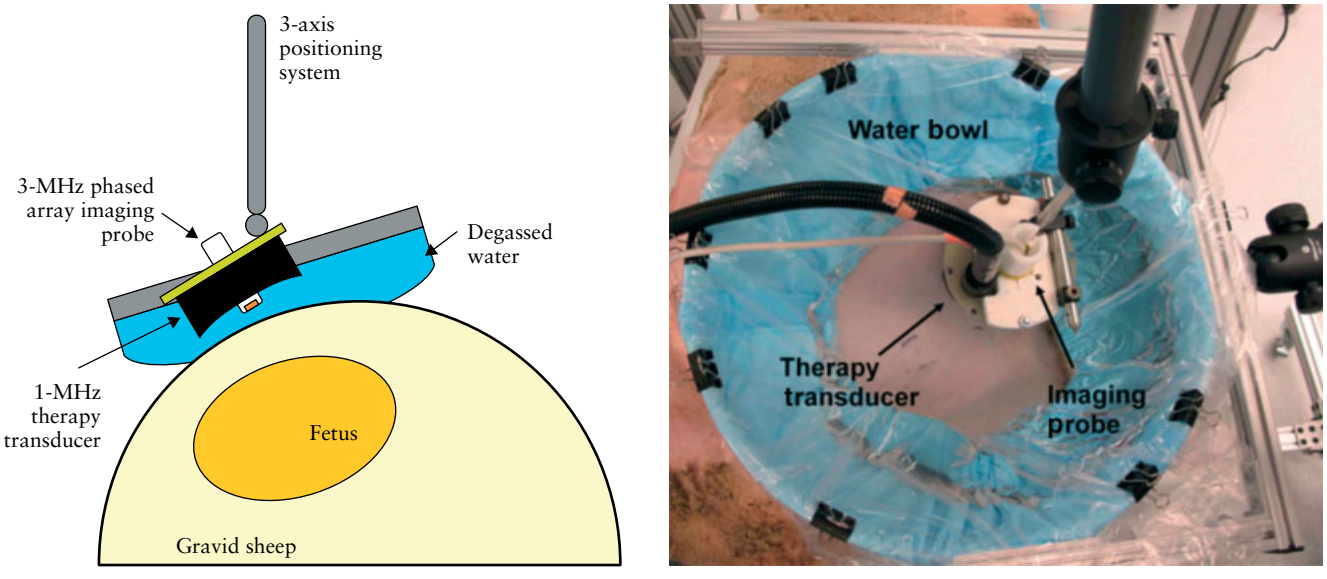

Figure 1 Diagram of the side view and photograph from above of the experimental set-up.

cloud serving the dual purpose of a tissue fractionation agent and a reference point for treatment guidance. 2D and color Doppler ultrasound imaging were used to follow the treatment and determine its effectiveness. Fetal kidney, liver, lung and heart were targeted at depths ranging from 2 to 8 cm from the maternal abdominal wall. In fetal kidney, liver and lung, cubic tissue volumes (0.1–1 cm^3) were targeted by mechanically scanning the focus of the therapeutic transducer through a 3D grid of points during ultrasound exposure, with each point treated for ~2 s and adjacent points separated by 0.5–1.5 mm. In fetal hearts, single-focus lesions were created by targeting individual spots from 30 to 80 s.

Following the intervention, the ewes were euthanized with pentobarbital. The fetuses were harvested and visually inspected for any signs of collateral damage near the targeted fetal organs. Targeted organs were removed and evaluated by gross examination, with samples stained with hematoxylin and eosin (H&E) for histological analysis by a pathologist (J.E.W.).

RESULTS

A total of 19 of 31 treatment attempts resulted in the successful generation of a cavitation cloud at the target, with lesions observed in 17 of the 19 cases in which cavitation was generated (Table 1). Fetal kidney, liver and heart were primary targets, with fetal lungs treated on two occasions. Morphological and histological examination confirmed that lesions were generated at the sites where cavitation had been visualized on ultrasound imaging. No lesions were observed in targets where cavitation clouds were absent.

Cases with cavitating bubble cloud generation

Fetal kidney, liver and lung

Cavitating bubble clouds were observed in five of five treatments in kidney, five of nine treatments in liver and two of two treatments in lung, generating identifiable lesions in five kidneys, three livers and two lungs. In real time, the bubble clouds could be identified by their bright, flickering pattern, which was distinguishable from surrounding structures. The bubble clouds appeared as 3–4-mm-wide hyperechoic zones at the geometric focus of the transducer by 2D ultrasound imaging (Figure 2). On one occasion, the same liver was treated twice, with only one larger lesion found; the targeting locations of the two treatments were close enough that they likely formed a contiguous treated area which appeared as a single lesion. With the exception of one liver sample in which no clear signs of damage were encountered after treatment, lesions were present in all targets where cavitation bubble clouds were successfully generated.

Morphological inspection of fixed samples showed darkened hemorrhagic regions corresponding to the locations where the cavitation bubble clouds had been observed, with affected areas comparable in size to the dimensions of regions scanned during treatment (Figure 3a,d). Hemorrhage effects were noted to be more pronounced in the kidney than in other organs. Histological analysis revealed cellular destruction accompanied by hemorrhage within the treated area in the kidney and liver (Figure 3b,c,e,f), with similar lesion patterns observed in the lung (not shown). The damaged regions were filled with red blood cells, acellular debris and, in certain cases,

Table 1 Results of 31 attempts of pulsed cavitational ultrasound treatment of fetal sheep organs

Targeted organ	*Depth from maternal abdomen (cm)*	*Treatments with cavitation monitored at the target*	*Pathologically confirmed lesions in organs with cavitation*
Kidney	3.6 (2.7–5.6)	5/5 (100)	5/5 (100)
Liver	6.4 (2.4–8.2)	5/9 (56)	3/5 (60)
Lung	6.4 (5.8–7.0)	2/2 (100)	2/2 (100)
Heart	7.2 (3.9–8.2)	7/15 (47)	7/7 (100)
Overall	6.5 (2.4–8.2)	19/31 (61)	17/19 (89)

Data are given as median (range) or *n* (%).

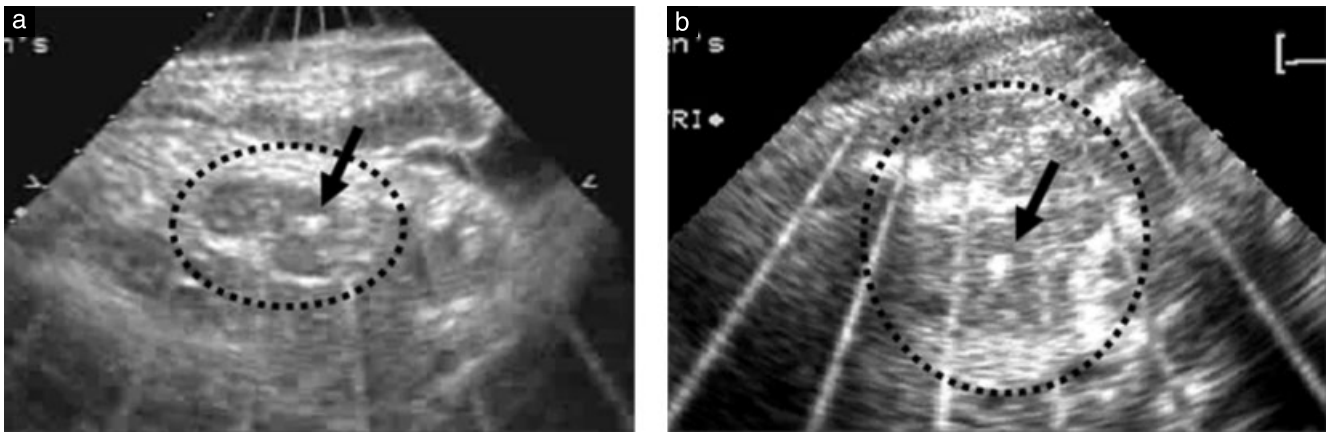

Figure 2 Two-dimensional ultrasound images of a fetal kidney (a) and liver (b) during therapeutic ultrasound exposure. Cavitation bubble clouds were created at the focus of the therapeutic transducer (arrows). The high-intensity pulses originating from the therapeutic transducer caused visible radial interference patterns in both images.

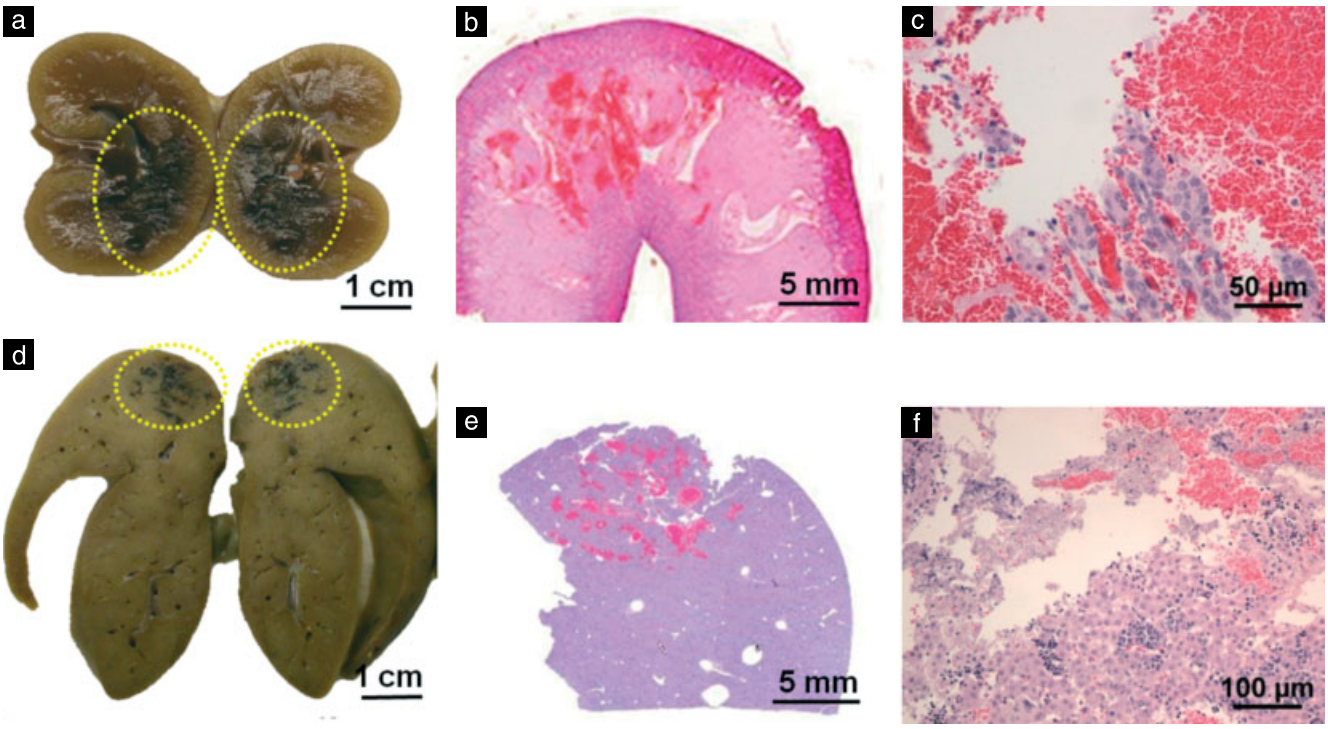

Figure 3 Representative pathology and histology pictures of a fetal kidney (a–c) and liver (d–f) treated by pulsed cavitational ultrasound. The dark regions indicated by the ellipses correspond to lesion areas created by mechanically scanning the treatment focus (a and d). Histological examination revealed interspersed hemorrhagic spots in both kidney and liver (b and e). Damaged areas consisted of a variable combination of red blood cells, subcellular debris and intact tissue cells (c and f).

isolated islands of intact cells. The degree of cellular disruption in the lesions varied from case to case, ranging from total loss of all normal tissue architecture and structures to primarily hemorrhage with the majority of cellular structures physically intact.

Fetal heart

Cavitation bubble clouds were successfully generated at the focus in seven of 15 fetal heart treatments. A total of seven targeted single focus lesions were verified by pathology: five in the ventricular septum and two in the ventricular wall. The ventricular free wall was specifically targeted in cases where the ventricular septum was deeper in the maternal abdomen than reachable by the focal zone of the therapy transducer.

In one case, a lesion created in the ventricular septum perforated the septum and resulted in a ventricular septal defect (VSD), confirmed by 2D and color Doppler echocardiography (Figure 4). Transient fetal bradycardia was observed during several treatments, but resolved spontaneously with cessation of treatment. In two separate cases, heart function ceased a few minutes after treatment. On both occasions, a cavitation cloud had been sustained for prolonged periods of time (60 s or more) in the basal portion of the heart, possibly in the vicinity of the atrioventricular node.

Morphology revealed discolored myocardium at sites where cavitating bubble clouds had been present. Lesions created in the ventricular septum were ~2–3 mm in diameter, corresponding to the diameter of the cavitation cloud. A small amount of hemorrhage on the exterior of the ventricular wall was observed in two of three fetal hearts where the ventricular septum had been targeted. In one case (not the VSD case), however, precise lesions were created in the ventricular septum while the heart's exterior remained intact with no damage visible outside the targeted region (Figure 5a,b). In treatments where the ventricular wall was targeted, lesions were accompanied by the presence of substantial superficial hemorrhage on the pericardium (Figure 5c,d).

Histological evaluation of the ventricular septum lesions showed complete fractionation of the septal tissue at the site of treatment with moderate amounts of free blood in the lesion (Figure 6a,b). The myocardial structure was completely lost in the majority of cases, with lesions characterized by sharp margins. Most of the defect was lined by eosinophilic, contracted myocytes, flanked by normal myocardium. In a few areas, there was a thin rim of cellular debris between the blood and the myocardium. Lesions created on the ventricular free wall were generally characterized by significant hemorrhage and cellular ablation (Figure 6c,d). In many areas, blood surrounded clusters of intact cardiomyocytes. Other areas had considerable cellular debris between the blood and the intact myocardium. Lesions that were less penetrating nevertheless consisted of hemorrhage and significant cellular destruction. Hemorrhage into the myocardial interstitium was occasionally present. The mildest lesions consisted of epicardial hemorrhage with small focal areas of cellular debris between the free blood and the myocardium.

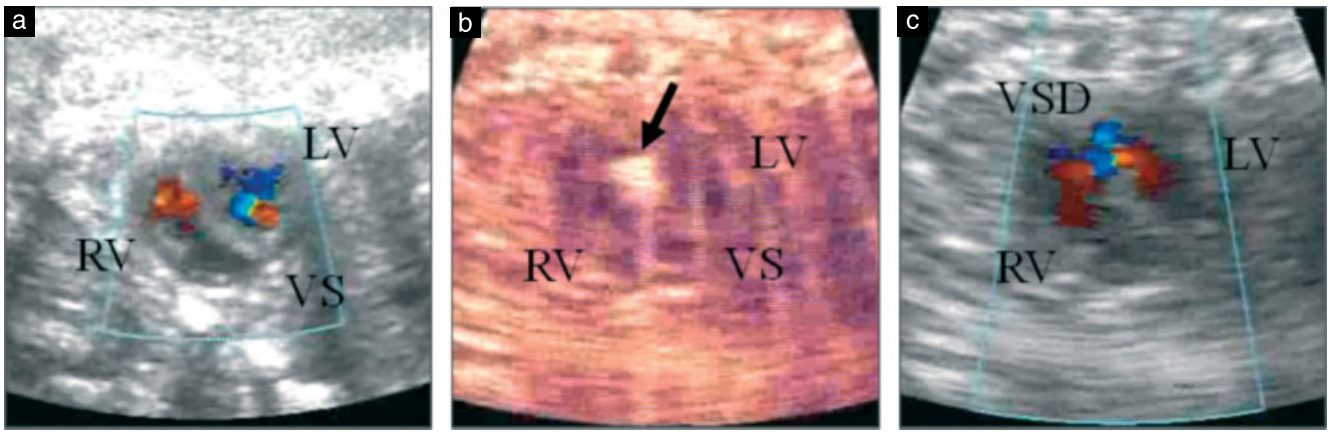

Figure 4 (a) Pretreatment color Doppler image of the fetal heart, showing an intact ventricular septum (VS). (b) A cavitation bubble cloud is seen as a hyperechoic zone during histotripsy application, as indicated by the arrow. (c) Post-treatment color Doppler image of the fetal heart. The creation of a ventricular septal defect (VSD) allows a flow channel between the left ventricle (LV) and the right ventricle (RV).

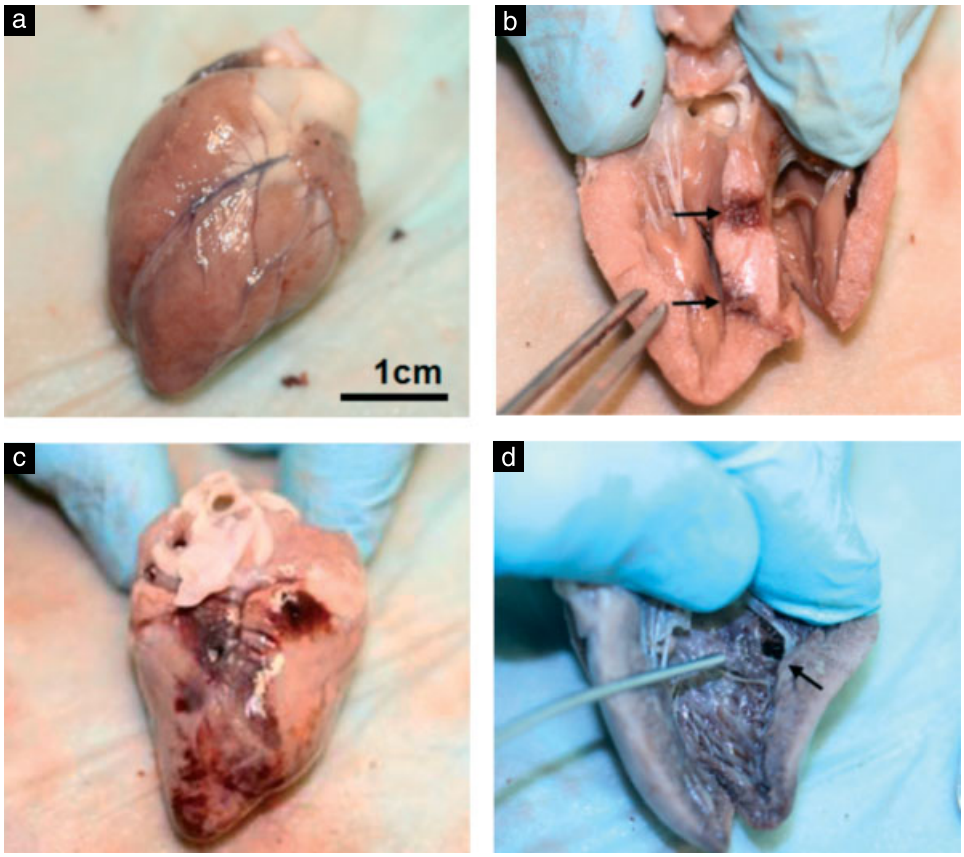

Figure 5 (a, b) A fetal heart in which the ventricular septum was targeted. (a) External view with intact exterior. (b) A longitudinal section of the heart revealed two lesions, created in the ventricular septum after 30 and 60 s of exposure (indicated by the arrows), of ~2 and 3 mm in diameter, respectively. The lesion edges were well defined within the ventricular septum, without noticeable damage outside this area. (c, d) Sample heart in which the ventricular wall was targeted. (c) Substantial superficial hemorrhage was present on the heart wall. (d) A lesion 3 mm in diameter (arrow) was generated after 80 s of treatment.

Cases without cavitating bubble cloud generation

Three factors were associated with the inability to generate a cavitating bubble cloud at the focus: depth of the target organ, acoustic obstruction by fetal limbs and the presence of prefocal cavitation (Table 2). A cavitating cloud was generated in 100% (6/6) of fetal targets <4 cm from the maternal abdominal surface (Figure 7); in targets >4 cm from the maternal abdominal surface, the success rate for generation of a bubble cloud was only 52% (13/25, $P = 0.06$). A fetal extremity was in the path of the ultrasound beam in 67% (8/12) of cases with unsuccessful generation of a cavitating cloud, but only 21% (4/19) of cases with successful cavitation generation ($P = 0.03$). In

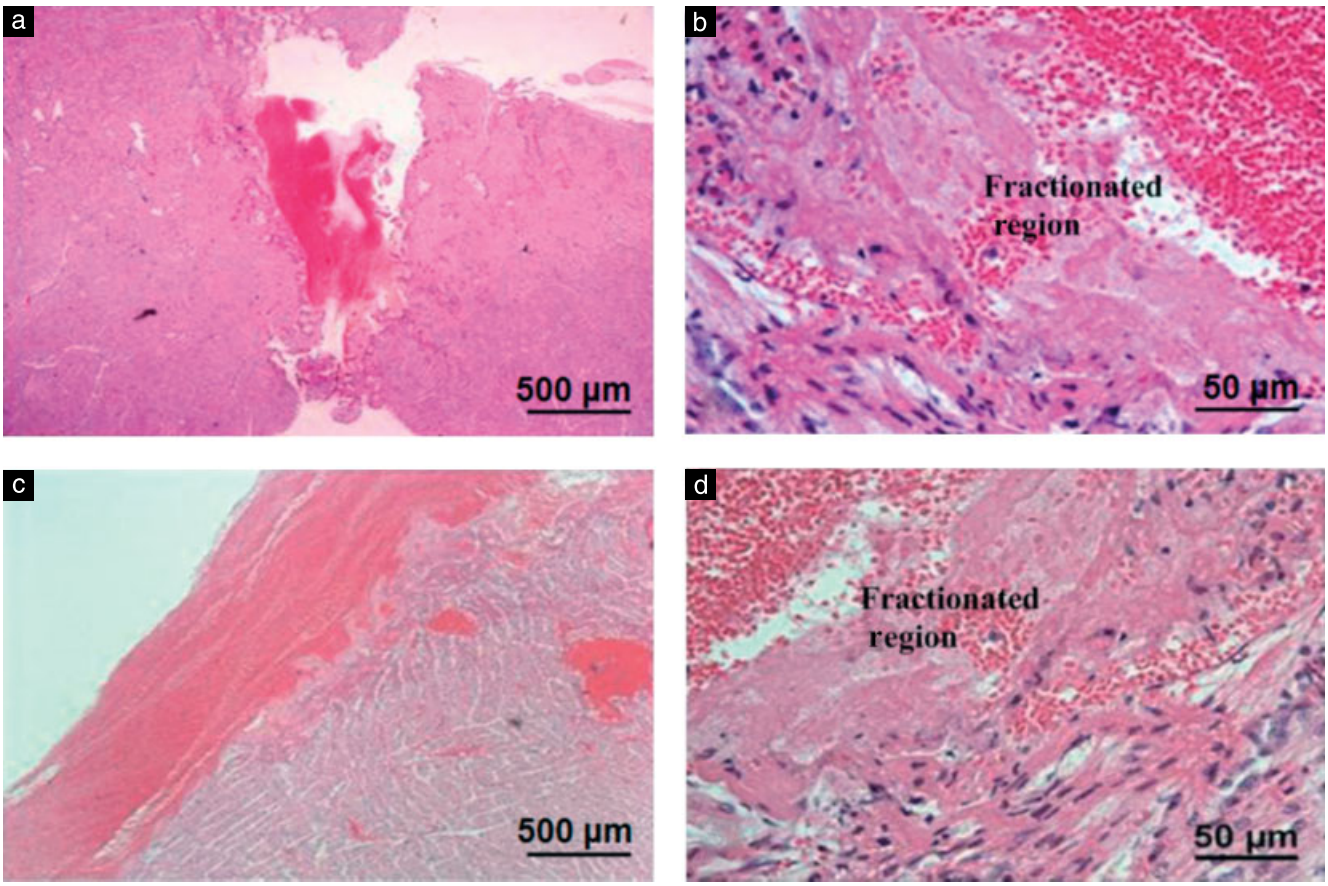

Figure 6 (a, b) Hematoxylin and eosin slides of a lesion created in the ventricular septum at × 2 (a) and × 20 (b) original magnification. (a) The darker area corresponds to residual blood from the ventricle that has coagulated inside the lesion cavity, which spanned almost the entire septum. (b) Fractionated areas were characterized by distinct boundaries. (c, d) Lesions created on the heart wall were accompanied by epicardial hemorrhage with mild tissue destruction, here shown at × 2 (c) and × 20 (d) original magnification.

Table 2 Predictors of cavitation generation

	Cavitation generated (n = 19)	*No cavitation generated (n = 12)*	P*
Gestational age (days)	112 (102–129)	119 (108–129)	0.76
Target depth (cm)	6.0 (2.4–7.7)	7.4 (4.5–8.2)	0.003
Fetal organ			0.11
Liver	5	4	
Kidney	5	0	
Heart	7	8	
Lung	2	0	
Fetal orientation			0.07
Spine up	9	2	
Spine down	3	4	
Right side up	1	4	
Left side up	6	2	
Obstructing structure†	7	10	0.05
Obstructing fetal limbs	4	8	0.03
Prefocal cavitation	7	9	0.04

Data are given as median (range) or *n*. *Mann–Whitney *U* test for categorical variables or Fisher's exact test for continuous variables. †Umbilical cord, placenta and fetal limbs.

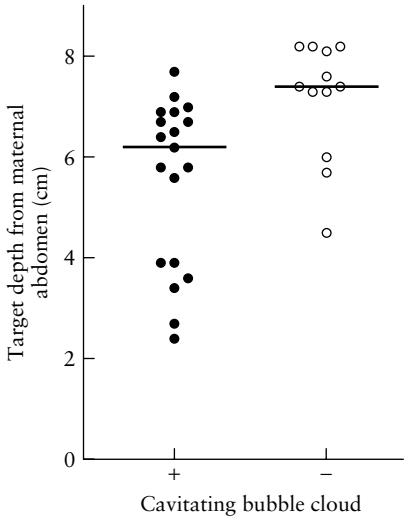

Figure 7 Incidence of focal cavitation according to target depth. Successful (●) and unsuccessful (○) attempts are shown. Horizontal lines indicate the median depth of each distribution.

52% (16/31) of the treatment cases, varying amounts of prefocal cavitation were observed at the fetal skin and amniotic fluid interface, reducing or completely blocking ultrasound energy from reaching the target. This effect was observed in 75% (9/12) of cases in which a bubble cloud could not be generated at the focus and in 37% (7/19) of cases in which a cloud was successfully generated ($P = 0.04$). In general, short-lived prefocal cavitation did

not create any visible damage to fetal tissues, but in a few lambs, longer and more intense occurrences caused partial discoloration on the fetal skin, possibly due to superficial hemorrhage.

DISCUSSION

In this study, extracorporeal histotripsy was used to successfully generate lesions in fetal targets. Treatment was guided by a temporally changing, hyperechoic cavitation bubble cloud at the site of lesion generation, which was monitored by ultrasound imaging.

Multiple fetal anomalies could benefit from a non-invasive, precise method of tissue destruction. Possible clinical applications in the human fetus include de-bulking of solid masses causing compression of vital structures or fetal distress, cardiac interventions such as creation of atrial septal defects or perforation of atretic valves, and selective reduction of multiple gestations via direct targeting of the fetal heart. In addition, given that significant bleeding has not been observed in other models after histotripsy therapy of vascular organs[14], even vascular structures and/or malformations (i.e. teratomas or communicating vessels in twin–twin transfusion syndrome and twin reversed arterial perfusion syndrome) could be clinical targets. Furthermore, previous studies have shown that high-intensity focused ultrasound can induce coagulation and hemostasis through thermal and cavitational means[16,17].

Histotripsy was successful in creating lesions in 17 of 31 treatment attempts. In kidney, liver and lung, the size of the affected regions was comparable with the dimensions of the treatment scan. There was increased flanking hemorrhage in the kidney, perhaps due to its high vascularity; however, ongoing studies show that hemorrhage and flanking injury induced by histotripsy recover within 1 month in neonatal porcine hearts (G.E. Owens, personal communication, June 17, 2010). The degree of cellular disruption in the lesions varied from total loss of all normal tissue architecture to primarily hemorrhage. This variability could be attributed to different levels of acoustic aberration and attenuation from fetal bone and tissue in each experiment. In heart treatments, 2–3-mm lesions separated by < 1 cm were generated within the fetal ventricular septum. Considering that the ultrasound beam had to traverse up to 8 cm of overlying tissue, this targeting accuracy surpassed our initial expectations, but still needs further refinement in order to improve consistency and to optimize ultrasound parameters for maximal tissue removal, which was not done in this feasibility study.

Because treatment accuracy is determined by the cavitation bubble cloud size at the target, which depends on acoustic parameters and therapy transducer characteristics, parameter optimization and transducer design modifications could increase the accuracy of the treatment. Improving echocardiographic imaging guidance quality by incorporating a high-resolution curvilinear imaging transducer in the system would also be beneficial and is currently under development.

Unsuccessful experiments were more likely to have overlying limbs, commonly with increased depth to target. These are somewhat predictable associations, as bone obstruction and multiple layers of inhomogeneous media will invariably subject the ultrasound beam to high degrees of attenuation and aberration before it reaches the focus. Attenuation makes it difficult to achieve sufficiently high focal pressures to initiate cavitation, while acoustic aberration effects may change the focal pressure profile and increase the pressure levels of secondary lobes, decreasing targeting accuracy. To minimize these undesirable effects, choosing an appropriate acoustic window with minimal bone and tissue in the pathway is needed prior to treatment. The use of more powerful therapeutic transducers could also help compensate for attenuation effects in deep-seated targets, and aberration correction mechanisms could be applied to refocus the transducer to an extent by using phased array systems[18,19]. However, implementation for *in vivo* applications involves significant technical obstacles that were beyond the scope of this study. Another possibility is treatment at earlier gestational stages, when fetal bones are less calcified. The aberration and attenuation from overlying fetal bone and tissue would be lower, although higher treatment accuracy would be required due to the smaller overall size of the fetus and targets.

An additional challenge is the animal model. Although sheep are commonly used in non-clinical fetal studies, particular characteristics of this model have added to the challenges in our experiments. In humans, the uterus is located directly beneath the maternal abdomen, making the fetus accessible and somewhat amenable to manipulation. In comparison, maneuverability of the fetal sheep is limited by a bicornuate uterus and multiple fetuses, while ultrasound access is impaired by overlying maternal bowel. Fetal lambs also have proportionally large limbs and hooves, which calcify at a relatively early gestational age[20], limiting the availability of treatment windows. Fetal wool also increases the likelihood of prefocal cavitation events. Although these particular difficulties would not be present in a clinical scenario, other variables such as movement of the fetus and greater fetal depth would need to be addressed.

Concern has been raised that fractionated tissue debris resulting from histotripsy therapy may become hazardous emboli. An *in vitro* study has been conducted to assess the size distribution of these tissue debris particles[21]. Results showed no presence of particles > 60 μm in diameter, with $> 80\%$ of the particles < 6 μm. Such particles are unlikely to form hazardous emboli, because 100-μm mechanical filters have been successful at preventing embolization in catheter-based thrombolysis procedures[22]. However, it is not known what size particles in a fetus can cause significant embolization. To further investigate the embolization risk, we plan to perform postprocedure diffusion-weighted MRI and pathology analysis of fetal

organs including the brain, lungs and kidneys in future experiments.

This feasibility study in the sheep model demonstrated that extracorporeal histotripsy therapy can induce localized tissue fractionation in fetal organs. These initial results demonstrate the potential of this technique, but it is clear that fetal histotripsy will require further refinement in order to become a viable tool for fetal intervention applications. Future studies will focus on improving the treatment consistency and accuracy in order to demonstrate the safety and efficacy of the technology.

REFERENCES

1. Heron M, Hoyert DL, Murphy SL, Xu J, Kochanek KD, Tejada-Vera B. Deaths: final data for 2006. *Natl Vital Stat Rep* 2009; **57**: 1–134.
2. Selamet Tierney ES, Wald RM, McElhinney DB, Marshall AC, Benson CB, Colan SD, Marcus EN, Marx GR, Levine JC, Wilkins-Haug L, Lock JE, Tworetzky W. Changes in left heart hemodynamics after technically successful *in-utero* aortic valvuloplasty. *Ultrasound Obstet Gynecol* 2007; **30**: 715–720.
3. Marshall AC, Levine J, Morash D, Silva V, Lock JE, Benson CB, Wilkins-Haug LE, McElhinney DB, Tworetzky W. Results of *in utero* atrial septoplasty in fetuses with hypoplastic left heart syndrome. *Prenat Diagn* 2008; **28**: 1023–1028.
4. McElhinney DB, Tworetzky W, Lock JE. Current status of fetal cardiac intervention. *Circulation* 2010; **121**: 1256–1263.
5. De Lia JE, Kuhlmann RS, Harstad TW, Cruikshank DP. Fetoscopic laser ablation of placental vessels in severe previable twin–twin transfusion syndrome. *Am J Obstet Gynecol* 1995; **172**: 1202–1211.
6. Grethel EJ, Wagner AJ, Clifton MS, Cortes RA, Farmer DL, Harrison MR, Nobuhara KK, Lee H. Fetal intervention for mass lesions and hydrops improves outcome: a 15-year experience. *J Pediatr Surg* 2007; **42**: 117–123.
7. Paek BW, Vaezy S, Fujimoto V, Bailey M, Albanese CT, Harrison MR, Farmer DL. Tissue ablation using high-intensity focused ultrasound in the fetal sheep model: potential for fetal treatment. *Am J Obstet Gynecol* 2003; **189**: 702–705.
8. Paek BW, Foley J, Zderic V, Starr F, Shields LE, Vaezy S. Selective reduction of multifetal pregnancy using high-intensity focused ultrasound in the rabbit model. *Ultrasound Obstet Gynecol* 2005; **26**: 267–270.
9. Xu Z, Mekhala R, Hall TL, Chang C, Mycek M, Fowlkes JB, Cain CA. High speed imaging of bubble clouds generated in pulsed ultrasound cavitational therapy – histotripsy. *IEEE Trans Ultrason Ferroelectr Freq Control* 2007; **54**: 2091–2101.
10. Parsons J, Cain CA, Abrams GD, Fowlkes JB. Pulsed cavitational ultrasound therapy for controlled tissue homogenization. *Ultrasound Med Biol* 2006; **32**: 115–129.
11. Fowlkes JB, Crum LA. Cavitation threshold measurements for micro-second length pulses of ultrasound. *J Acoust Soc Am* 1988; **83**: 2190–2201.
12. Xu Z, Ludomirsky A, Eun LY, Hall TL, Tran BC, Fowlkes JB, Cain CA. Controlled ultrasound tissue erosion. *IEEE Trans Ultrason Ferroelectr Freq Control* 2004; **51**: 726–736.
13. Xu Z, Gordon D, Owens G, Cain C, Ludomirsky A. Noninvasive creation of an atrial septal defect by histotripsy in a canine model. *Circulation* 2010; **121**: 742–749.
14. Hall TL, Kieran K, Ives K, Fowlkes JB, Cain CA, Roberts WW. Histotripsy of rabbit renal tissue *in vivo*: temporal histologic trends. *J Endourol* 2007; **21**: 1159–1166.
15. Lake AM, Hall TL, Kieran K, Fowlkes JB, Cain CA, Roberts WW. Histotripsy: minimally invasive technology for prostatic tissue ablation in an *in vivo* canine model. *Urology* 2008; **72**: 682–686.
16. Vaezy S, Martin R, Mourad P, Crum L. Hemostasis using high intensity focused ultrasound. *Eur J Ultrasound* 1999; **9**: 79–87.
17. Poliachik SL, Chandler WL, Mourad PD, Ollos RJ, Crum LA. Activation, aggregation and adhesion of platelets exposed to high-intensity focused ultrasound. *Ultrasound Med Biol* 2001; **27**: 1567–1576.
18. Wang H, Ebbini ES, O'Donnell M, Cain CA. Phase aberration correction and motion compensation for ultrasonic hyperthermia phased arrays: experimental results. *IEEE Trans Ultrason Ferroelectr Freq Control* 1994; **41**: 34–43.
19. Thomas J-L, Fink MA. Ultrasonic beam focusing through tissue inhomogeneities with a time reversal mirror: application to transskull therapy. *IEEE Trans Ultrason Ferroelectr Freq Control* 1996; **43**: 1122–1129.
20. Ahmed NS. Development of forelimb bones in indigenous sheep fetuses. *Iraqi J Vet Sci* 2008; **22**: 87–94.
21. Xu Z, Fan Z, Hall TL, Winterroth F, Fowlkes JB, Cain CA. Size measurement of tissue debris particles generated from mechanical tissue fractionation by pulsed cavitational ultrasound therapy – histotripsy. *Ultrasound Med Biol* 2009; **35**: 245–255.
22. Eskandari M. Cerebral embolic protection. *Semin Vasc Surg* 2005; **18**: 95–100.

